Spontaneous Synthesis of [Fe^{II}(Atrz)$_3$]SO$_4$ and its Analogues Through Accelerated Ageing: New Insights from Small-Scale Reactions

Rhona F. Lonergan,[a] Georgina A. Conway,[a] Patrick W. Doheny,[a] and Helena J. Shepherd*[a]

Abstract: Accelerated ageing reactions that take place between two solid materials on contact in the absence of added solvent have been used to synthesize two spin-crossover-active 1D coordination polymers and one of their Cu(II) analogues. The hygroscopy of the ligands and the relative humidity of the reaction chamber have been shown to be particularly important factors in the rate of reaction. Small-scale reactions between a few individual crystals have allowed observation of deliquescence of the 4-aminotriazole ligand at high humidity. The metal salt does not dissolve, and the ligand diffuses into the crystal of the metal salt during the reaction. In the case of the Cu analogue, the formation of the product causes the crystal of the metal salt to deform with the formation of pseudocrystals, which have a fibrous structure.

Introduction

The search for cleaner, greener synthesis of the materials we rely on in everyday life, as well as for the technologies of the future, is a major concern within the chemical sciences. Key strategies for achieving this include minimizing the number of synthetic steps, employing catalytic processes, reduction of energy consumption and reducing the amount of hazardous waste produced, which includes solvents. One approach to achieve this is mechanochemistry, which involves the use of mechanical force to accomplish chemical transformations, many of which would otherwise be achieved through more traditional solution-state processes.[1] Mechanochemical reactions involve very little (if any) solvent, substantially reducing waste, and can also eliminate any solubility or stoichiometry problems that can prevent recovery of a product in solution-state reactions[2] and as a result can lead to significant increases in yield.[3]

Friščić et al. defines accelerated aging (AA) reactions as "diffusion-controlled reactions that take place between initially solid reactants, and are accelerated or directed by only mild or short-lasting changes in their environment."[4] These reactions are a further extension of the rationale behind mechanochemistry methods. AA reactions take advantage of the inherent mobility of molecules and further reduce the energy require-ments of the reaction whilst retaining all of the benefits of mechanochemistry. As suggested by the name, the initial direction of AA research has been inspired by reactions present in the natural world such as mineral weathering,[5] geological biomineralization,[6] and mineral neogenesis,[7] which take place over long periods of time. Over the last fifteen years, the true potential of AA reactions has become apparent, as the technique has been developed to synthesize zeolitic imidazo-late frameworks (ZIFs),[5,7] metal–organic frameworks (MOFs),[8] nanoparticles,[9] and co-crystals,[10,11] as well as being used in catalysis[12] and staple organic reactions such as Micheal addition.[13] The hygroscopy of starting materials has been shown to be an important factor in the viability of some AA reactions[14] where, for example, in relation to the synthesis of co-crystals,[14] the very hygroscopic malonic acid forms co-crystals with caffeine but adipic and succinic acid (which are much less hygroscopic) do not. This emphasis on the hygro-scopy of the starting materials indicates that the deliquescence of at least one starting material is an important aspect in the mechanism of AA reactions. High relative humidity (RH) has also been shown to be beneficial in several reactions[5–7,10–13] and, in some cases, evidence shows that the rate of reaction is humidity dependent.[10,11,15] There are several reports of reac-tions not proceeding at low RH (e.g., below < 30% RH), slow or incomplete reactions at moderate RH (e.g., ~50%) and fast reactions with full conversion at high RH (e.g., > 70% RH).[10,14] In some cases, additives such as ammonium sulphate have been used to control the rate of reactivity or control product formation.[5]

As Friščić et al. have discussed, the time scales and relative simplicity of AA reaction design can provide a useful platform for mechanistic studies that may have wider ranging implica-tions for other reaction types including mechanochemistry.[4] An increase in reaction rate that results from reduced particle size has been shown,[6,16] and a device for monitoring of AA reactions in situ using powder X-ray diffraction has also been

[a] R. F. Lonergan, G. A. Conway, Dr. P. W. Doheny, Dr. H. J. Shepherd
School of Physical Sciences
University of Kent
Giles Lane, Canterbury, CT2 7NZ (UK)
E-mail: h.j.shepherd@kent.ac.uk

Chemistry–A European Journal

Research Article
doi.org/10.1002/chem.202201823

Chemistry Europe
European Chemical
Societies Publishing

demonstrated.[17] An optical microscopy study of an organic co-crystallization AA reaction demonstrated the importance of humidity, adding a deliquescent material to the reagents to facilitate the dissolution of reactants from atmospheric water.[18] Solid-state NMR[19] and Raman spectroscopy[20] have also been integrated into the AA reaction to gain mechanistic insight. This report focusses on the use of optical microscopy to gain mechanistic insight into the synthesis of the spin crossover (SCO)-active material [Fe^{II}(Atrz)$_3$]SO$_4$ and its analogues.

While AA has been used to make supramolecular materials such as MOFs and ZIFs, to the best of our knowledge, no instances of the use of this method to synthesize stimuli-responsive materials have been reported. SCO complexes are a promising class of smart material which can switch between high spin (HS) and low spin (LS) states upon application of external stimuli such as changes in temperature, light irradiation or pressure.[21–23] This change in spin state is often accompanied by a dramatic change of color as well as changes to the magnetic and structural properties. The binary nature of these changes makes SCO materials suitable for a wide variety of applications such as temperature or pressure sensors,[24] as the active material in optical displays[25] and even in actuator devices.[26–28] The simple and scalable nature of AA reactions as well as the low-cost of the starting materials make these reactions even more suited for these large-scale applications.

4-substituted 1,2,4-triazoles are a simple and versatile family of ligands, which are often used in coordination chemistry and in the synthesis of MOFs[29] but they also have interesting properties and uses as organic materials. For example, these ligands/molecules have been used in the creation of OLEDs, organic photovoltaic cells and data storage devices.[30] 1,2,4-triazoles have several commercially available derivatives as well as relatively simple synthetic pathways for more complex derivatives,[31] which makes them an easily accessible starting material for large-scale commercial applications. They are used in a ubiquitous family of one-dimensional SCO-active iron(II) triazole coordination polymers, of general formula [Fe(R-trz)$_3$]·A$_2$ (where R = substituent at 4-position, A = anion), as shown in Scheme 1. The triple triazole bridges in these polymers act as rigid but stable linkages due to a lack of strain with a large family of these materials known.[31] They exhibit attractive SCO properties, often featuring abrupt transitions (where the SCO occurs over a few Kelvin), wide hysteresis (i.e., the temperature of the transition on cooling is lower than that on warming, creating a form of molecular memory), and high-temperature operation (> 300 K).[31,32] Recent work has also shown the significant potential for post-synthetic modification to alter the R-group of the triazole in the final SCO material.[43] This further expands the library of triazole functionalities that can be incorporated into these compounds, which in turn widens the tunability of the SCO properties of these 1D
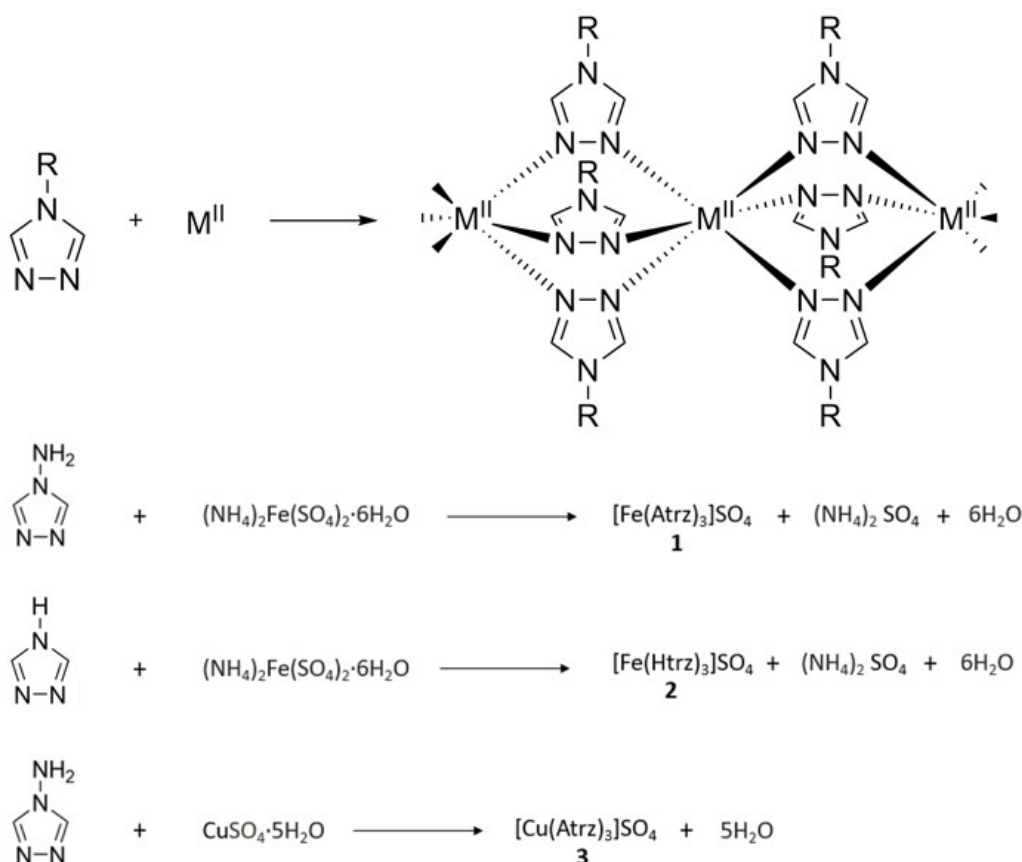
Scheme 1. Structure and general reaction scheme for the synthesis of the 1D [M(R-trz)$_3$]$^{2+}$ coordination polymers and the synthesis of compounds **1**–**3**.

Chemistry–A European Journal

Research Article
doi.org/10.1002/chem.202201823

Chemistry Europe
European Chemical
Societies Publishing

polymers. Despite the substantial advantages of $[Fe(R\text{-}trz)_3]\cdot A_2$ systems, a significant drawback is that they are notoriously difficult to crystallize.[31] As a consequence, relatively few solid-state structures of these systems have been published from powder diffraction data,[33,34] with even fewer determined via single crystal diffraction.[35] Until recently, the best evidence for their 1D chain structure was by examination of Cu analogues, $[Cu(R\text{-}trz)_3]\cdot A_2$, which have a much higher propensity for growth of single crystals.[36]

There are currently several different methods for synthesis of $[Fe(R\text{-}trz)_3]\cdot A_2$ materials. The first is the addition of the two starting materials in solution as established by Króber et al., in 1994.[37] Similar solution-state methods have since been used to access a range of related materials.[31,38] The reverse micelle technique has been used to create SCO-active iron(II) triazole nanoparticles (NPs)[39–42] and flow chemistry has also been used to synthesize iron(II) triazole NPs, allowing fine control over particle size, but requiring specialized experimental setups.[43,44] More recently, these iron triazole polymers have been synthesized 'direct from the metal' using zero valent iron as the metal precursor to form the complex in a one-step reaction.[45] Mechanochemistry has also been used to synthesize these metal triazole systems.[8,46,47] This method removes any solubility problems, increasing the yield, and is quick and simple, with reaction times of minutes instead of hours or days. However, additional washing is needed to obtain samples of high purity. Another method currently in use for the synthesis of these materials, is post-synthetic modification of products made using the previously described methods either mechanochemically[46] or in solution.[48] This allows access to analogues containing different anions and variations of the triazole ligands that could not previously be synthesized ab initio, but it also adds an additional step in the synthetic process and shares the same problems as their respective parent methods. The synthetic route to these materials is particularly important considering the sensitivity of their switching properties to particle size, solvent, matrix effects and preparation techniques.[49,50]

Here, we show the synthesis of the SCO-active compounds $[Fe(Atrz)_3]SO_4$ (**1**), $[Fe(Htrz)_3]SO_4$ (**2**) and the Cu analogue of **1**, $[Cu(Atrz)_3]SO_4$ (**3**) (Atrz = 4-amino-1,2,4-triazole, Htrz = 4H-1,2,4-triazole) via accelerated aging. The aim is to determine if functional SCO materials may be synthesized using AA methods, and more importantly, to gain mechanistic insights into the AA process. The reaction schemes for compounds **1**–**3** are shown in Scheme 1. The solution-state synthesis of compound **1** has been previously reported to show a reversible spin transition at 355 K, with a thermal hysteresis of 32 K.[51] This compound has also been synthesized mechanochemically, showing similar SCO properties to the solution-synthesized material.[8] High quality powder diffraction combined with Rietveld refinement has previously produced a crystal structure for compound **1**[45] while compounds **2**, and **3** have not previously been reported in the literature.

Results and Discussion

Contact between crystalline Atrz and Mohr's salt in the absence of solvent results in the direct formation of compound **1**, as shown in Figure 1(a). The formation of the purple product, which is typical of this family of Fe-triazole materials in the LS state, from the colorless starting materials is readily visible, and this has been used to follow the reaction as a function of time using optical reflectivity measurements, *vide infra*. Time-lapse recordings of the reactions used to synthesize compounds **1**–**3** on this bulk-scale can be found in the Supporting Information, Videos 1–3.

Successful synthesis of **1** was confirmed via a Le Bail fit of the powder diffraction pattern of the washed product with those of the starting materials and the previously reported crystal structure,[45] as shown in Figure 2(a). The as-synthesized product is contaminated with ammonium sulphate, which is a by-product of the reaction. A simple washing step as described in the experimental section removes this contamination to yield a pure sample of **1**. SQUID magnetometry (Figure 2b) indicates an abrupt reversible spin transition which is accompanied by a hysteresis of 12 K ($T_{1/2}\uparrow = 342$ K, $T_{1/2}\downarrow = 330$). This is very similar to the values obtained for the previously-reported solution-state[34] and mechanochemically-synthesized materials.[8] Thermal analysis via TGA/DSC (Figure S1) shows SCO occurring as expected on warming. A mass loss of approximately 5% at 390 K is attributed to the dehydration of the sample followed by
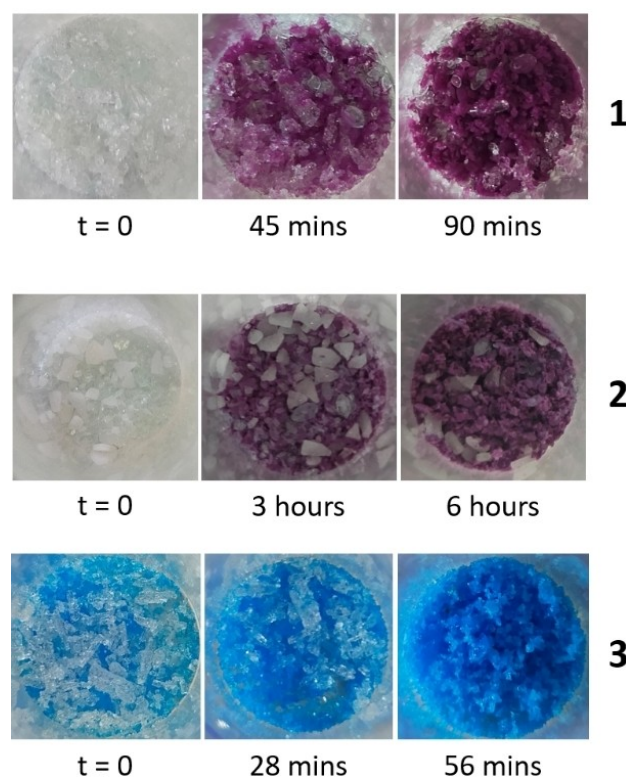

Figure 1. Photographs showing the formation of compounds **1**, **2** and **3** as a function of time after mixing of solid reagents ($t = 0$) at 99% RH and 23 °C. The reaction vessel is 19 mm in diameter in each case.

Chemistry–A European Journal

Research Article
doi.org/10.1002/chem.202201823

Chemistry Europe
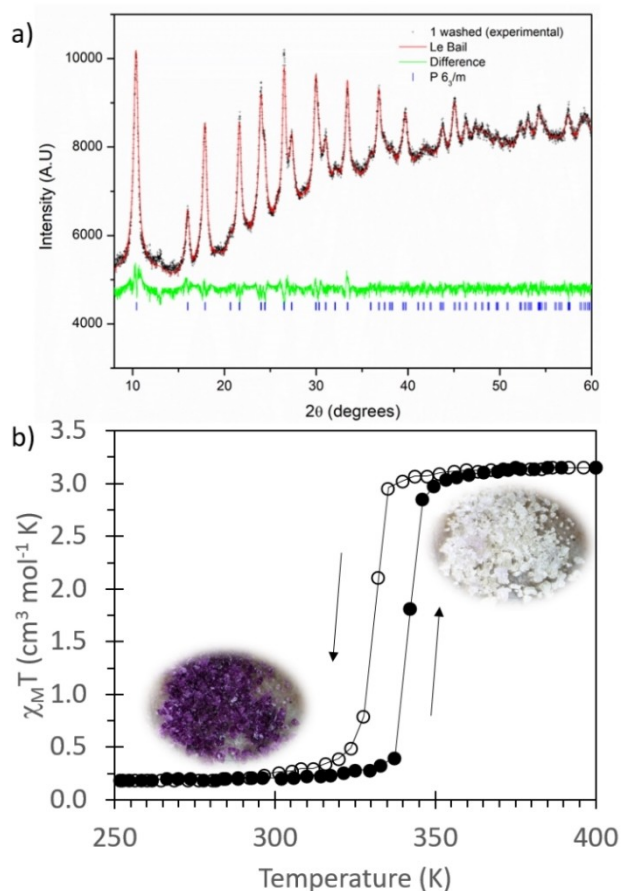European Chemical
Societies Publishing

Figure 2. a) Powder diffraction pattern and Le Bail fit of **1**, b) SQUID magnetometry of **1** showing a hysteretic spin transition. Inset shows a polycrystalline sample of **1** in the LS (purple) and HS (white) states.

Figure 3. a) Powder diffraction patterns of **1** and **2**, b) SQUID magnetometry of **2** showing an irreversible spin transition on heating from room temperature. Inset shows a polycrystalline sample of **2** below (purple) and above (brown) the irreversible transition.

decomposition above 550 K. The similarity of the powder diffraction pattern of **1** to that of the known anhydrous material implies that this water is physically adsorbed onto the surface of the product rather than incorporated into the crystal structure. Comparison of the powder diffraction pattern and the magnetometry to the reported literature of this previously characterized compound clearly confirms that compound **1** has been successfully synthesized simply by placing the solid reagents into contact in this AA reaction.

Compounds **2** and **3** were also synthesized in an analogous manner to compound **1**, as shown in Figure 1. Again, characteristic color changes can be observed in each case as the reaction progresses, videos of which can be found in the Supporting Information (Videos 2 and 3). Neither compound **2** nor **3** have been previously reported and so comparison of their properties to literature values is not possible. However, a Le Bail fit of powder X-ray diffraction data of **3** to the known unit cell of **1** revealed them to be structural analogues of each other (Figure S9). A comparison of the powder X-ray diffraction patterns of compounds **1** and **2**, as shown in Figure 3a, reveals that they are not structurally analogous. This is perhaps not surprising given the significant differences in structure of the Atrz and Htrz complexes formed with iron tetrafluoroborate,
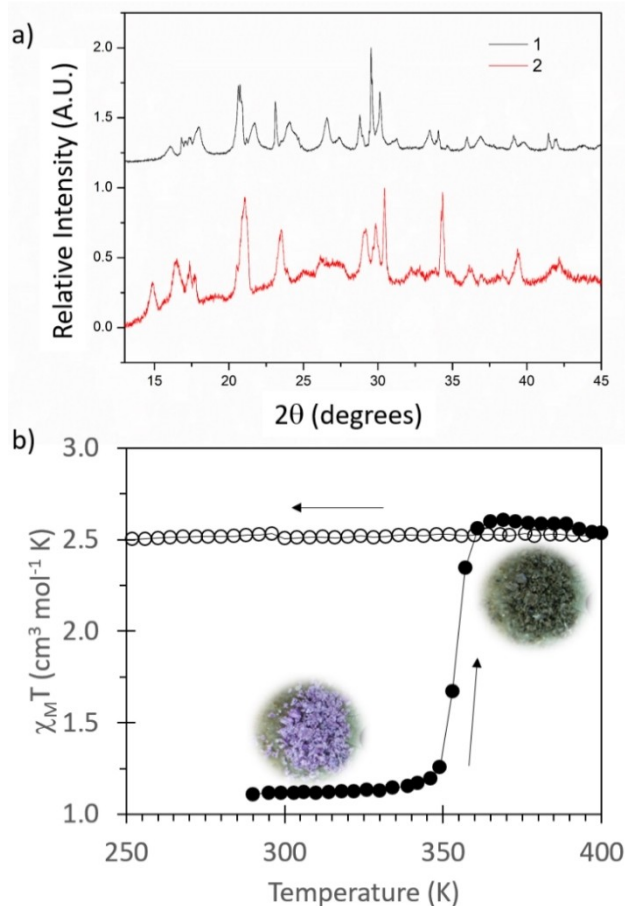
which have been thoroughly investigated.[31] While compound **3** (Cu^{2+}, d^9) is not expected to be SCO-active, compound **2** presents an irreversible SCO centered at 355 K on heating, as shown in Figure 3(b). The spin transition is accompanied by a color change from purple to a grey/brown. The HS state of these materials is typically white, suggesting that this color change may be the result of sample decay, which also prevents the reverse spin transition. While heating to lower temperatures was attempted in order to prevent decomposition, we were unable to observe a reversible transition for compound **2**. Further information regarding the characterization of **2** and **3**, including thermal analysis can be found in the Supporting Information.

Beyond the SCO properties of compounds **1** and **2**, the primary interest in these materials here is that they allow insights into the effect of varying both the ligand and the metal salt on the AA reaction itself. For example, Htrz, used in the synthesis of **2**, is much less hygroscopic than Atrz. Furthermore, Cu(II) triazole complexes such as **3** have been shown to form single crystals more readily than their Fe(II) analogues,[36] raising the possibility of synthesizing single crystals using AA methods.

Chemistry–A European Journal

Research Article
doi.org/10.1002/chem.202201823

Chemistry Europe
European Chemical
Societies Publishing

The relative hygroscopies of Htrz and Atrz were evaluated by comparing the mass of water they adsorb from a 99% RH environment as a function of time, as shown in Figure 4(a). Atrz fully deliquesces at this humidity, absorbing almost 1.5 molar equivalents of water over 24 h, while Htrz does not deliquesce on this timescale, absorbing less than 0.5 molar equivalents. By contrast, copper sulphate crystals absorbed very little atmospheric water at all. After an initial adsorption of 0.1 molar equivalents within the first hour, ammonium iron sulphate also absorbed very little atmospheric water. The increase in hygroscopy on moving from Atrz to Htrz is reflected in the increased rate of reaction for **1** when compared to that of **2**, as shown in Figure 4(b). The effect of relative humidity on the formation of **1** and **2** was also evaluated using reflectivity measurements, as shown in Figure 4(c and d). As RH increases, the reaction occurs more quickly, supporting the positive correlation between RH and reactivity that has been previously noted in other AA reactions.[5–7,10–13] Ammonium sulphate, which is a byproduct of synthesis of both **1** and **2** has previously been used as a catalyst in the AA synthesis of various ZIF compounds.[5] In the interests of determining if ammonium sulphate may also be contributing to the reactivity through increased hygroscopy, the reaction of Atrz with iron sulphate was also investigated, as described in the Supporting Information. The reaction with ammonium iron sulphate to form **1** indeed proceeded more quickly than that with iron sulphate and so it is possible that the ammonium sulphate is accelerating the rate of reaction.

The reaction to form compound **3** was the most rapid, although this increase in reaction rate compared to formation of compound **1** cannot be attributed to differences in hygroscopy of the starting materials alone as copper sulphate and ammonium iron sulphate have comparable uptake of atmospheric water. Consequently, we tentatively attribute the increased reactivity to inherent differences in the stabilities of the iron- and copper-containing products. The curves shown in Figure 4 give an indication as to the relative rate of formation of each product based on the appearance of the colored product as a function of time. Recording of these curves, particularly for rapid reactions is somewhat complicated by differences in ambient humidity that the reagents are subjected to whilst weighing and mixing and thus detailed kinetic analysis is not possible. The results of repeated reactions to form compound **1** at various humidities is shown in the Supporting Information Figure S4.

The role of solvent vapors on the crystallinity, morphology and spin crossover properties of SCO-active thin films has previously been investigated for a molecular complex.[52] It was shown that above a specific threshold RH water, and indeed other solvents, were able to recrystallize the films in situ, modifying their properties. In this context, it is also worth adding that evidence of reactivity for compounds **1**, **2** and **3** has been observed in atmospheres of other solvents including dichloromethane and acetone, but not in ethanol in the case of **1** and **2**. We are currently investigating the role of different solvents on the mechanisms and rates of these reactions, as well as on the crystallinity of the final product.
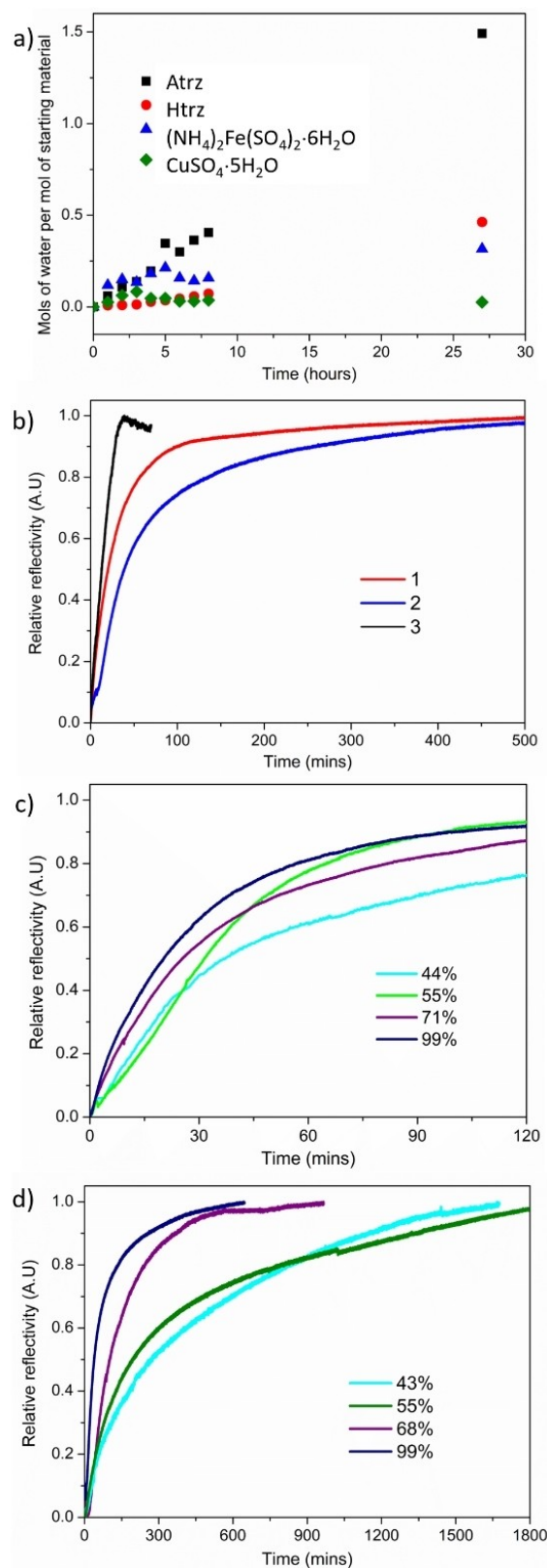

Figure 4. a) Proportion of water gained by each reagent as a function of time at 99% RH. b) Normalized reflectivity measurements showing the formation of compounds **1**–**3** as a function of time at 99% RH. c) Effect of RH on rate of reaction for compound **1**. d) Effect of RH on rate of reaction for compound **2**. Note the different timescales for (c) and (d).

Chemistry–A European Journal

Research Article
doi.org/10.1002/chem.202201823

Chemistry
Europe
European Chemical
Societies Publishing

In an effort to further investigate the mechanisms behind the AA processes occurring in the formation of these metal-triazole complexes, reactions were carried out on a smaller scale, between individual crystals. Due to the difficulties associated with accurately determining the mass of individual crystals, particularly those which are highly hygroscopic, it is not possible to accurately control the stoichiometry of such reactions and as such the products may contain a significant amount of unreacted starting materials. However, these small-scale reactions are an opportunity to observe the processes occurring during AA, a vital step towards controlling and exploiting this reaction mechanism.

The formation of **1** from a single crystal of Atrz and a single crystal of $(NH_4)_2Fe(SO_4)_2 \cdot 6H_2O$ is shown in Figure 5(a), and Video 4, where the crystals are both colorless prior to reaction. At 0 minutes they are first brought into contact, and within a few minutes the Atrz crystal becomes noticeably smaller and a sheen of condensation is apparent surrounding the crystals. This is accompanied by development of the purple color that is characteristic of **1** in the LS state, within the region of the $(NH_4)_2Fe(SO_4)_2 \cdot 6H_2O$ crystal only. As time progresses, an envelope of water forms around the reagents and the Atrz crystal completely deliquesces. At no point does the $(NH_4)_2Fe(SO_4)_2 \cdot 6H_2O$ crystal dissolve, demonstrating that this is not a concentrated solution-state reaction as has been previously observed for some AA co-crystallization reactions involving deliquescence.[18] Instead, the formation of **1** proceeds at the site of the crystal of the metal salt. On further standing the water envelope dries and no further changes are observed. The remaining purple solid is similar in shape to the crystal of the Fe salt starting material but is significantly larger and is no longer a single crystal, breaking into small microcrystalline

fragments in response to even small, externally applied forces. Clearly, the reaction is occurring at the site of the metal salt, with ligand molecules (in this instance dissolved in water) reacting with the metal salt. On the bulk scale it was seen that no unreacted starting materials remain in the product and so it can be assumed the ligand diffuses into the crystal of the metal salt, destroying its integrity as a single crystal as it does so. It should however be noted that these iron-containing coordination polymers are notoriously difficult to grow single crystals of, and the powder-like nature of the product may be intrinsic to this class of material rather than a result of the AA process.

The reaction was repeated to form compound **2**, with a similar sized single crystal of $(NH_4)_2Fe(SO_4)_2 \cdot 6H_2O$ and a few crystals of Htrz (necessary due to the smaller crystallite size of this starting material and a desire to preserve broadly similar stoichiometry between the two reactions). As shown in Figure 5(b) and Video 5, no condensation of atmospheric water can be observed at ambient humidity, and the reaction proceeds much more slowly than in the case of **1**. Careful inspection of the images reveals the formation of the purple product, **2**, only at the interfaces in which the crystals are in direct contact. These areas are highlighted with arrows in the final panel of Figure 5(b). From this, it can be concluded that the increased hygroscopy and resultant deliquescence of Atrz allows for much more rapid diffusion of the ligand onto, and indeed into, the metal salt crystal. As was shown previously in the case of bulk materials, the rate of formation of both **1** and **2** can be significantly increased as RH increases, and thus the optimal humidity for any given AA reaction is liable to be highly dependent on the hygroscopy of the specific starting materials.

The reaction between copper sulphate and Atrz was also carried out on a single crystal scale to produce **3**, as shown in
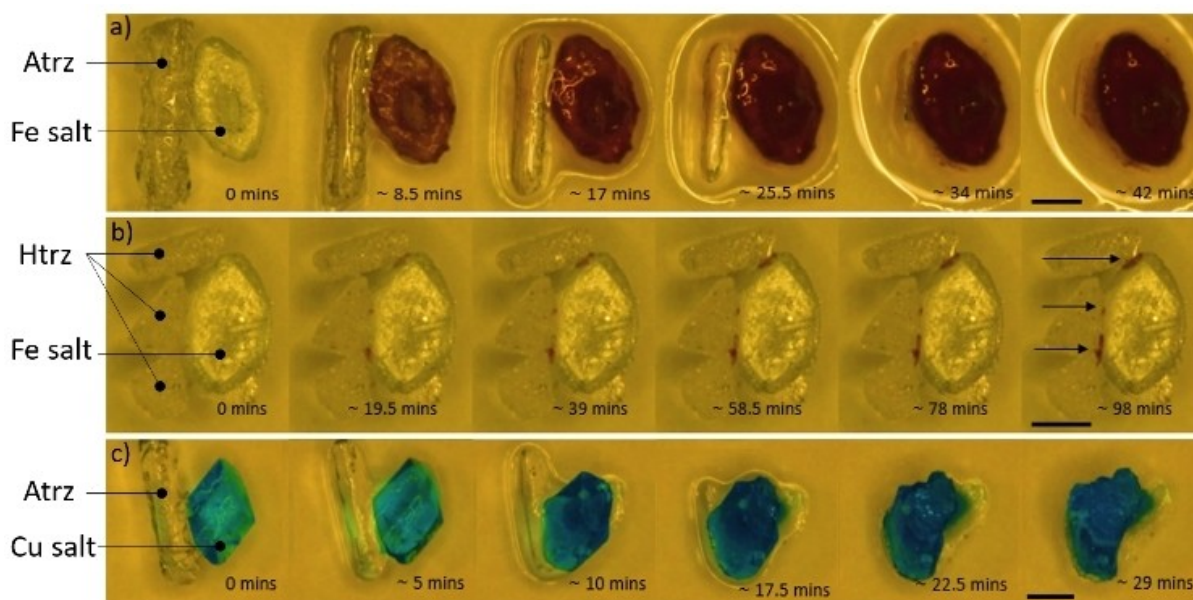

Figure 5. Images showing reactions between single crystals of the metal salts and triazole ligands as a function of time to afford compounds (a) **1**, (b) **2** and (c) **3**. Arrows in the final panel of (b) highlight areas of product formation as described in the text. The scale bar represents 1 mm, all experiments were conducted at ambient temperature and humidity.

Chemistry–A European Journal

Research Article
doi.org/10.1002/chem.202201823

Chemistry Europe
European Chemical
Societies Publishing

Figure 5(c) and in supporting Video 6. Formation of the product is indicated through the appearance of the dark blue product from colorless and pale blue starting materials. In a similar manner to the analogous small-scale synthesis of the iron-containing analogue, **1**, the Atrz crystal deliquesces and an envelope of water forms around the crystals during the reaction, allowing for the rapid synthesis of **3**. Again, at no point does the crystal of the metal salt dissolve during the reaction. However, unlike in the case of **1**, the shape of the solid remaining after the reaction looks significantly different from the initial crystal of the metal salt. The small-scale synthesis of **3** was repeated several times, including with an excess of Atrz to ensure a complete reaction, as shown in Figures 6(a) and S11. At high and low humidities the product formed tends to be polycrystalline and disintegrates on the application of pressure, as was seen in the formation of compound **1**. However, at intermediate humidities around 55% RH, a pseudocrystal is formed. A pseudocrystal is an object that appears crystalline when observed with a microscope but does not produce the diffraction pattern associated with a single crystal. The shape of this pseudocrystal is very different to the parent copper sulphate crystal, with numerous cracks and regions of it having expanded significantly and splayed outward. When viewed under a polarizing microscope with the polarizer and analyzer crossed, the pseudocrystal **3** transmits light, as would be expected from a single crystal (Figure 6b). On rotation of a section of the pseudocrystal perpendicular to the plane of the polarizers, the transmitted light extinguishes every 90°, again showing optical activity expected from an ordered crystalline material rather than an amorphous glass or polycrystalline agglomerate. While the parent copper sulphate crystal has the diffraction pattern expected from a single crystal, the diffraction pattern of a pseudocrystal of compound **3** shows a pattern more usually associated with diffraction from a fibrous material. Diffraction patterns of both the parent copper sulphate crystal and the pseudocrystalline compound **3** are shown in Figure 6(c) and (d), respectively.

Representative SEM microscopy of two pseudocrystals of compound **3** is shown in Figure 7. The overall appearance of each object shows a multitude of cracks, undulations, and growths from the surface. Baleen-like fibrous structures are visible as growths from the surface of the pseudocrystal shown in Figure 7(a and b). The pseudocrystal in Figure 7(c) had been cut in half prior to imaging and Figure 7(d) shows that the internal structure also features fibrous regions as evidenced by the diffraction pattern. EDX measurements reveal the presence of carbon and nitrogen throughout the cross-section of the pseudocrystal, indicating complete ligand penetration throughout the product, which was formerly the single crystal of the metal salt, as shown in Figure S10. Fibrous or rod-like morphologies have been previously observed for $[Fe(R\text{-}trz)_3]\cdot A_2$ complexes[53,54] and is possibly related to their anisotropic 1D coordination polymer structure. Further investigations into the nature of these fibers and their possible relationship to the crystallographic orientation of the parent crystal of the metal salt is underway.

In addition to the hygroscopy of the starting materials, there are several other factors that may influence the rate of these AA reactions. In this case, the starting materials for both the bulk- and small-scale reactions were not ground prior to use in order to allow optimal imaging of the ligand and metal salt during the reaction. However, particle size and efficient mixing of reagents in the solid state has already been shown to have a significant effect on the rate of reaction,[6,16] and it is
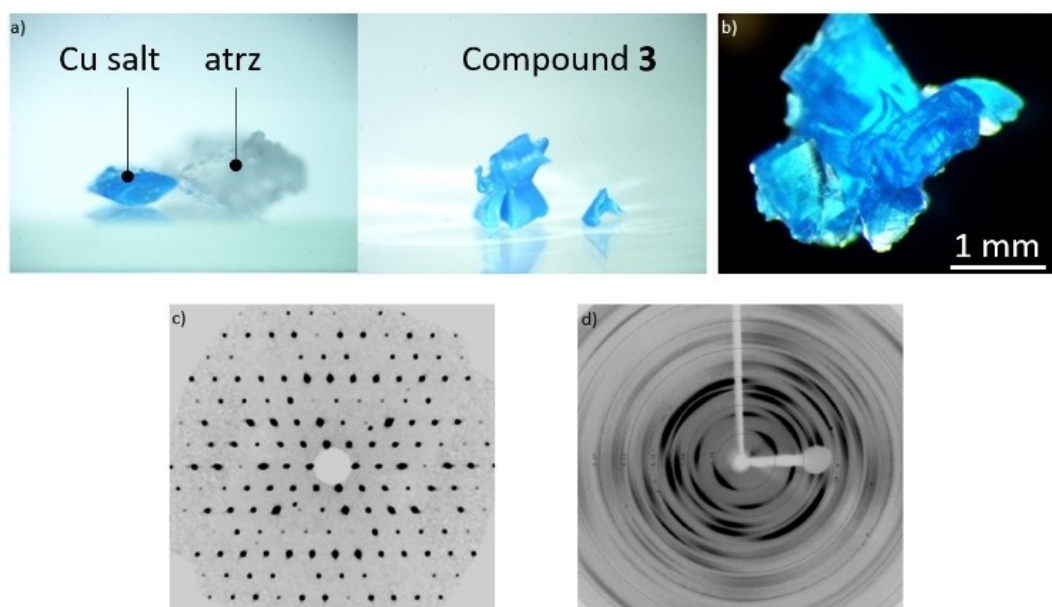

Figure 6. a) Side view of copper sulphate and Atrz crystals before reaction and then of compound 3 after the reaction at 55% RH, b) a pseudocrystal of compound 3 imaged between crossed polarizers, demonstrating its ability to transmit plane-polarized light c) a reconstruction of the hk0 plane from the copper sulphate starting material and d) diffraction pattern of compound **3**.
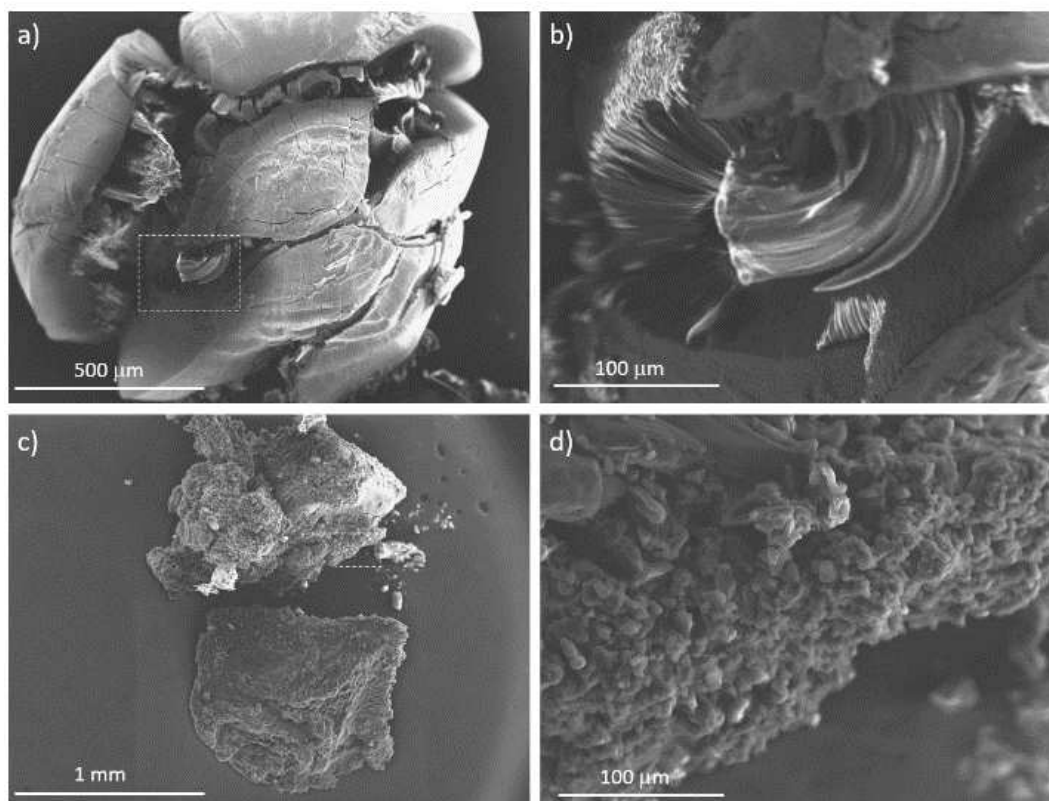
Chemistry–A European Journal

Research Article
doi.org/10.1002/chem.202201823

Chemistry Europe
European Chemical
Societies Publishing

Figure 7. SEM images of two pseudocrystals of 3 showing evidence of fibrous formations. Highlighted region in a) corresponds to the region imaged in b), highlighted region in c) corresponds to the same region imaged in d).

likely that similar results would be found here. Relative crystallographic orientations of the individual crystallites may also influence the rate of the reaction at smaller scales, particularly in cases where the ligand does not fully deliquesce. While a number of other factors may influence the rate of the reaction, the observation of the product forming at the site of the parent metal salt is important and deserves further investigation on a range of coordination polymers and metal–organic framework materials.

Conclusion

We have shown that compounds **1**–**3** can be synthesized via accelerated ageing through contact of the starting materials in a humid environment in the absence of added solvent and without grinding of either the reagents or the reaction mixture. The formation of products with a color that is distinctive from the starting materials allows the reactions to be imaged in situ and reaction progress to be quantified using reflectivity measurements. Compounds **1** and **2** both show spin crossover properties in the solid state. The role of humidity in facilitating the reactions has been demonstrated and it is seen that the relative hygroscopy of the ligands in particular is an important factor in determining the rate of the reaction.

Using time-dependent optical microscopy, small-scale reactions between single crystals of the starting materials have allowed crucial insights into the mechanism of the accelerated ageing process for the first time. In all cases, the formation of the product takes place at the site of the metal salt, with ligand molecules diffusing into the crystal. This results in significant expansion of the crystal as the product is formed, and in the case of compound **3**, a pseudocrystal may be produced. While these pseudocrystals appear crystalline using polarizing microscopy, they have been shown to be fibrous in nature. These results are expected to have significant implications for the interpretation of solvent-free syntheses of coordination polymers and related framework materials and demonstrates the importance of optical microscopy measurements in mechanistic studies.

Experimental Section

Bulk-scale synthesis: All reagents were purchased from Fisher Scientific and used as received. All accelerated aging reactions at the bulk scale were carried out with a 1:3 metal salt:1,2,4-triazole ligand stoichiometric ratio, typically on the scale of 1.30 mmol of metal with 3.90 mmol of ligand (ca. 0.1 g to 0.3 g). The reagents were combined before being gently shaken and left uncovered, either under ambient conditions or at specific relative humidities (~ 37 %, 55 %, 70 % and 99 %), to react for 24 h. An air-tight humidity

Chemistry–A European Journal

Research Article
doi.org/10.1002/chem.202201823

Chemistry Europe
European Chemical
Societies Publishing

chamber was built from a repurposed desiccator with a flat plate glass window to allow monitoring of reaction progress using a microscope and camera. Relative humidity within the chamber was controlled using binary salt solutions[55] and monitored using a Tempo Disc Bluetooth wireless smart sensor inside the chamber. Images of the reaction were recorded every 3–10 seconds after mixing using a Brinno TLC200 Pro time-lapse camera. Data analysis was performed using ImageJ,[56] where each image was converted to grey scale and an average grey value was extracted within a specified region of interest containing the sample. A background correction was applied to negate the automatic white balance adjustments of the camera. Data were normalized between 0 and 1 to obtain values representing relative change in darkness of the sample as a function of time and inverted such that 1 is the darker colored end of the scale, corresponding to the formation of product. ImageJ was also used to create the time-lapse videos as shown in the Supporting Information.

Samples were then analyzed without any further experimental steps. Selected samples were then washed gently with water to remove impurities. Washing of individual samples is always clearly indicated in the relevant figure. The samples produced through this bulk synthesis method were used for TGA/DSC, SQUID magnetometry, PXRD and elemental analysis.

Caution: Compound 3 undergoes high energy decomposition at high temperatures, extreme caution should be taken when heating.

Single crystal synthesis: Single crystals of each starting material were placed in contact at ambient conditions (~40% RH, ~19°C) on a glass slide. They were left open to air for the duration of the experiment and were monitored using a stereo microscope equipped with a digital camera. Images were captured every 3 seconds. ImageJ was used to create time-lapse videos as shown in the Supporting Information.

Hygroscopy of reagents: The hygroscopy of the starting materials was investigated by determining the mass of the materials immediately after opening the reagent bottle. They were then placed into a humidity chamber at 99% RH and their mass was measured at regular intervals. This data was used to calculate the molar proportion of water adsorbed as a function of time.

SQUID Magnetometry: The samples were loaded into gelatin capsules and placed into plastic straws with a uniform diamagnetic background. Magnetic susceptibility measurements were performed using a Quantum Design MPMS SQUID magnetometer. Temperature dependent measurements were made using a 1000 Oe magnetic field across the stated temperature ranges (in sweep mode), while ramping the temperature at 2 K/min.

Elemental analysis: Elemental analyses were conducted through the Elemental Analysis Service at London Metropolitan University using a ThermoFlash 2000 analyser.

Diffraction data: Powder XRD data were collected on a Rigaku Miniflex 600 using a Cu radiation source and measurements were performed at room temperature. Le Bail fits[57] were performed using the Rietica[58] software with an automatic smoothed background function. Diffraction data used to generate images shown in Figure 6 were collected on a Rigaku Oxford Diffraction Super-Nova S2 single crystal diffractometer using a Cu radiation source. The fibre-like diffraction image of the pseudocrystal of compound 3 was collected using a 10 degree phi scan.

SEM/EDX: SEM images were collected using a Hitachi S-3400 microscope. Samples were fixed to a carbon mount and scanned without sputtering.

Conflict of Interest

The authors declare no conflict of interest.

Data Availability Statement

The data that support the findings of this study are available from the corresponding author upon reasonable request.

[1] S. L. James, C. J. Adams, C. Bolm, D. Braga, P. Collier, T. Friščić, F. Grepioni, K. D. M. Harris, G. Hyett, W. Jones, et al., *Chem. Soc. Rev.* **2012**, *41*, 413–47.
[2] J. L. Do, T. Friščić, *ACS Cent. Sci.* **2017**, *3*, 13–19.
[3] G. T. Tigineh, L. Liu, *J. Chin. Chem. Soc.* **2019**, *66*, 1729–1737, jccs. 201800486.
[4] I. Huskić, C. B. Lennox, T. Friščić, *Green Chem.* **2020**, *22*, 5881–5901.
[5] M. J. Cliffe, C. Mottillo, R. S. Stein, D. K. Bučar, T. Friščić, *Chem. Sci.* **2012**, *3*, 2495–2500.
[6] F. Qi, R. S. Stein, T. Friščić, *Green Chem.* **2014**, *16*, 121–132.
[7] C. Mottillo, Y. Lu, M. H. Pham, M. J. Cliffe, T. O. Do, T. Friščić, *Green Chem.* **2013**, *15*, 2121–2131.
[8] J. H. Askew, H. J. Shepherd, *Chem. Commun.* **2018**, *54*, 180–183.
[9] M. Y. Malca, H. Bao, T. Bastaille, N. K. Saadé, J. M. Kinsella, T. Friščić, A. Moores, *Chem. Mater.* **2017**, *29*, 7766–7773.
[10] A. Jayasankar, A. Somwangthanaroj, Z. J. Shao, N. Rodríguez-Hornedo, *Pharm. Res.* **2006**, *23*, 2381–2392.
[11] I. Sarceviča, L. Orola, K. P. Nartowski, Y. Z. Khimyak, A. N. Round, L. Fábián, *Mol. Pharm.* **2015**, *12*, 2981–2992.
[12] D. Cinčić, I. Brekalo, B. Kaitner, *Chem. Commun.* **2012**, *48*, 11683–11685.
[13] S. Nakamatsu, S. Toyota, W. Jones, F. Toda, *Chem. Commun.* **2005**, 3808–3810.
[14] K. P. Nartowski, Y. Z. Khimyak, D. J. Berry, *CrystEngComm* **2016**, *18*, 2617–2620.
[15] X. Chen, J. G. Stowell, K. R. Morris, S. R. Byrn, *J. Pharm. Biomed. Anal.* **2010**, *51*, 866–874.
[16] A. Y. Ibrahim, R. T. Forbes, N. Blagden, *CrystEngComm* **2011**, *13*, 1141–1152.
[17] I. Huskić, J. C. Christopherson, K. Užarević, T. Friščić, *Chem. Commun.* **2016**, *52*, 5120–5123.
[18] A. Jayasankar, D. J. Good, N. Rodríguez-Hornedo, *Mol. Pharm.* **2007**, *4*, 360–372.
[19] V. S. Mandala, S. J. Loewus, M. A. Mehta, *J. Phys. Chem. Lett.* **2014**, *5*, 3340–3344.
[20] D. Gracin, V. Štrukil, T. Friščic̈, I. Halasz, K. Užarevic̈, *Angew. Chem. Int. Ed.* **2014**, *53*, 6193–6197; *Angew. Chem.* **2014**, *126*, 6307–6311.
[21] O. Kahn, *Curr. Opin. Solid State Mater. Sci.* **1996**, *1*, 547–554.
[22] H. L. C. Feltham, S. Brooker, *Coord. Chem. Rev.* **2014**, *276*, 1–33.
[23] G. Molnár, M. Mikolasek, K. Ridier, A. Fahs, W. Nicolazzi, A. Bousseksou, *Ann. Phys.* **2019**, *531*, 1900076.
[24] J. Linares, E. Codjovi, Y. Garcia, *Sensors* **2012**, *12*, 4479–4492.
[25] G. Molnár, S. Rat, L. Salmon, W. Nicolazzi, A. Bousseksou, *Adv. Mater.* **2018**, *30*, 1703862.
[26] M. D. Manrique-Juárez, S. Rat, L. Salmon, G. Molnár, C. M. Quintero, L. Nicu, H. J. Shepherd, A. Bousseksou, *Coord. Chem. Rev.* **2016**, *308*, 395–408.
[27] S. Rat, V. Nagy, I. Suleimanov, G. Molnár, L. Salmon, P. Demont, L. Csóka, A. Bousseksou, *Chem. Commun.* **2016**, *52*, 11267–11269.

Chemistry–A European Journal

Research Article
doi.org/10.1002/chem.202201823

Chemistry Europe
European Chemical
Societies Publishing

[28] H. J. Shepherd, I. A. Gural'skiy, C. M. Quintero, S. Tricard, L. Salmon, G. Molnár, A. Bousseksou, *Nat. Commun.* **2013**, *4*, 2607.

[29] K. Kobalz, M. Kobalz, J. Möllmer, U. Junghans, M. Lange, J. Bergmann, S. Dietrich, M. Wecks, R. Gläser, H. Krautscheid, *Inorg. Chem.* **2016**, *55*, 6938–6948.

[30] A. Diaz-Ortiz, P. Prieto, J. R. Carrillo, R. Martin, I. Torres, *Curr. Org. Chem.* **2015**, *19*, 568–584.

[31] O. Roubeau, *Chem. Eur. J.* **2012**, *18*, 15230–15244.

[32] Y. C. Chuang, C. T. Liu, C. F. Sheu, W. L. Ho, G. H. Lee, C. C. Wang, Y. Wang, *Inorg. Chem.* **2012**, *51*, 4663–4671.

[33] N. Pittala, F. Thétiot, S. Triki, K. Boukheddaden, G. Chastanet, M. Marchivie, *Chem. Mater.* **2017**, *29*, 490–494.

[34] A. Grosjean, P. Négrier, P. Bordet, C. Etrillard, D. Mondieig, S. Pechev, E. Lebraud, J. F. Létard, P. Guionneau, *Eur. J. Inorg. Chem.* **2013**, *2*, 796–802.

[35] A. Grosjean, N. Daro, B. Kauffmann, A. Kaiba, J.-F. Létard, P. Guionneau, *Chem. Commun.* **2011**, *47*, 12382.

[36] Y. Garcia, P. J. Van Koningsbruggen, G. Bravic, P. Guionneau, D. Chasseau, G. L. Cascarano, J. Moscovici, K. Lambert, A. Michalowicz, O. Kahn, *Inorg. Chem.* **1997**, *36*, 27, 6357–6365.

[37] J. Króber, J.-P. Audiére, R. Claude, E. Codjovi, O. Kahn, J. G. Haasnoot, F. Groliére, C. Jay, A. Bousseksou, J. Linares, et al., *Chem. Mater.* **1994**, *6*, 1404–1412.

[38] L. G. Lavrenova, O. G. Shakirova, *Eur. J. Inorg. Chem.* **2013**, *2013*, 670–682.

[39] E. Coronado, J. R. Galán-Mascarós, M. Monrabal-Capilla, J. García-Martínez, P. Pardo-Ibáñez, *Adv. Mater.* **2007**, *19*, 1359–1361.

[40] T. Forestier, S. Mornet, N. Daro, T. Nishihara, S. Mouri, K. Tanaka, O. Fouché, E. Freysz, J.-F. Létard, *Chem. Commun.* **2008**, 4327–4329.

[41] L. Moulet, N. Daro, C. Etrillard, J.-F. Létard, A. Grosjean, P. Guionneau, *Magnetochemistry* **2016**, *2*, 10.

[42] H. J. Shepherd, G. Molnár, W. Nicolazzi, L. Salmon, A. Bousseksou, *Eur. J. Inorg. Chem.* **2013**, *2013*, 653–661.

[43] K. Robertson, P. B. Flandrin, H. J. Shepherd, C. C. Wilson, *Chim. Oggi-Chem. Today* **2017**, *35*, 19–22.

[44] N. Daro, T. Vaudel, L. Afindouli, S. Marre, C. Aymonier, G. Chastanet, *Chem. Eur. J.* **2020**, *26*, 16286–16290.

[45] V. Y. Sirenko, O. I. Kucheriv, A. Rotaru, I. O. Fritsky, I. A. Gural'skiy, *Eur. J. Inorg. Chem.* **2020**, *2020*, 4523–4531.

[46] J. H. Askew, H. J. Shepherd, *Dalton Trans.* **2020**, *49*, 2966–2971.

[47] D. Nieto-Castro, F. A. Garcés-Pineda, A. Moneo-Corcuera, B. Pato-Doldan, F. Gispert-Guirado, J. Benet-Buchholz, J. R. Galán-Mascarós, *Inorg. Chem.* **2020**, *59*, 7953–7959.

[48] A. Enríquez-Cabrera, K. Ridier, L. Salmon, L. Routaboul, A. Bousseksou, *Eur. J. Inorg. Chem.* **2021**, *2021*, 2000–2016.

[49] L. Salmon, L. Catala, *Comptes Rend. Chim.* **2018**, *21*, 1230–1269.

[50] M. B. Bushuev, D. P. Pishchur, I. V. Korolkov, K. A. Vinogradova, *Phys. Chem. Chem. Phys.* **2017**, *19*, 4056–4068.

[51] L. G. Lavrenova, O. G. Shakirova, V. N. Ikorskii, V. A. Varnek, L. A. Sheludyakova, S. V. Larionov, *Russ. J. Coord. Chem.* **2003**, *29*, 22–27.

[52] A. C. Bas, V. Shalabaeva, X. Thompson, L. Vendier, L. Salmon, C. Thibault, G. Molnár, L. Routaboul, A. Bousseksou, *Comptes Rend. Chim.* **2019**, *22*, 525–533.

[53] A. Tokarev, L. Salmon, Y. Guari, G. Molnár, A. Bousseksou, *New J. Chem.* **2011**, *35*, 2081–2088.

[54] A. Rotaru, I. A. Gural'skiy, G. Molnár, L. Salmon, P. Demont, A. Bousseksou, *Chem. Commun.* **2012**, *48*, 4163–4165.

[55] L. Greenspan, *Humidity Fixed Points of Binary Saturated Aqueous Solutions.*, **1977**.

[56] C. A. Schneider, W. S. Rasband, K. W. Eliceiri, *Nat. Methods* **2012**, *9*, 671–675.

[57] A. Le Bail, H. Duroy, J. L. Fourquet, *Mater. Res. Bull.* **1988**, *23*, 447–452.

[58] B. Hunter, *Int. Union Crystallogr. Comm. Powder Diffr. Newsl.* **1998**, *20*.